Larrue, J., Rigaud, M., Razaka, G., Daret, D., Demond-Henri, J., & Bricand, H. (1983) *Biochem. Biophys. Res. Commun. 112*, 242-249.
Lees, M. B., & Paxman, S. (1972) *Anal. Biochem. 47*, 174-192.
Linfield, W. M., Barauskas, R. A., Sivieri, L., Serota, S., & Stevenson, R. W. (1984) *JAOCS, J. Am. Oil Chem. Soc. 61*, 191-195.
Linfield, W. M., Serota, S., & Sivieri, L. (1985) *JAOCS, J. Am. Oil Chem. Soc. 62*, 1152-1154.
Maas, R. L., Turk, J., Oates, J. A., & Brash, A. R. (1982) *J. Biol. Chem. 257*, 7056-7062.
Marcus, A. J., Safier, L. B., Ullman, H. L., Brockman, M. J., Islam, N., Oglesby, T. D., & Gorman, R. R. (1984) *Proc. Natl. Acad. Sci. U.S.A.* 81, 903-906.
Mayer, B., Moser, R., Gleispach, H., & Kukovetz, W. R. (1986) *Biochim. Biophys. Acta 875*, 641-653.
Pawlowski, N. A., Scott, W. A., Andreach, M., & Cohn, Z. A. (1982) *J. Exp. Med. 155*, 1653-1664.
Rabinovitch, H., Durand, J., Rigaud, M., Mendy, F., & Breton, M. (1981) *Lipids 16*, 518-524.
Richards, C. F., Johnson, A. R., & Campbell, W. B. (1986) *Biochim. Biophys. Acta 875*, 569-581.
Sando, G. N., & Sando, K. M. (1986) *Fed. Proc., Fed. Am. Soc. Exp. Biol. 45*, 1946 (Abstract).
Schafer, A. I., Takayama, H., Farrell, S., & Gimbrone, M. A., Jr. (1986) *Blood 67*, 373-378.
Shasby, D. M., Shasby, S. S., Sullivan, J. H., & Peach, M. J. (1982) *Circ. Res. 51*, 657-661.
Stenson, W. F., Nickells, M. W., & Atkinson, J. P. (1983) *Prostaglandins 26*, 253-263.
Turk, J., Mass, R. L., Brash, A. R., Roberts, J., II, & Oates, A. (1982) *J. Biol. Chem. 257*, 7068-7076.
Vanderhoek, J. Y., Bryant, R. W., & Bailey, J. M. (1980) *J. Biol. Chem. 255*, 5996-5998.
Vanderhoek, J. Y., Kiesel, L., Naor, Z., Bailey, J. M., & Catt, K. Y. (1984) *Prostaglandins, Leukotrienes Med. 15*, 375-385.
Van Rollins, M., Aveldano, M. I., Sprecher, H. W., & Horrocks, L. A. (1982) *Methods Enzymol. 86*, 518-530.
Yamada, K., Okuyma, H., Endo, Y., & Ikezawa, H. (1977) *Arch. Biochem. Biophys. 193*, 291-289.
Yang, S.-Y., Cuebas, D., & Schulz, H. (1986) *J. Biol. Chem. 261*, 12238-12243.

Reversible Dissociation of the B873 Light-Harvesting Complex from *Rhodospirillum rubrum* G9+[†,‡]

Robin Ghosh,[§] Helmut Hauser,[∥] and Reinhard Bachofen*[,§]
Institute for Plant Biology, Zollikerstrasse 107, CH-8008 Zürich, Switzerland, and Laboratory for Biochemistry, Universitätsstrasse 16, ETH-Zentrum, CH-8092 Zürich, Switzerland
Received December 1, 1986; Revised Manuscript Received September 28, 1987

ABSTRACT: The light-harvesting complex (B873) from the carotenoid-less mutant *Rhodospirillum rubrum* G9+ was isolated and used for studying the detergent-induced reversible changes in absorption and circular dichroism (CD) spectra. Addition of lauryldimethylamine *N*-oxide (LDAO) to the detergent-free B873 causes a rapid loss of the absorption maximum at 873 nm with the concomitant appearance of an absorption maximum at 775 nm. The absorption change is completely reversible by dilution of the LDAO-solubilized B873 into detergent-free buffer and is partially reversible by the addition of sodium cholate to a final concentration of 1% (w/v). Similar changes are observed by using near-IR CD, although no changes of secondary structure were seen by using UV CD. Detergent-free B873 dissolved in 0.2% octylpentakis-(oxyethylene) (O-POE) shows an absorption maximum principally at 873 nm and was shown by analytical ultracentrifugation measurements to exist as tetramers and hexamers (24-37K). O-POE concentrations above 0.5% cause the 873- to 780-nm transition described above to occur, and this is always associated with the formation of dimers (13K) and monomers (6.5K) containing bound bacteriochlorophyll. ESR studies performed with *N*-ethylmaleimide nitroxide labeled B873 dissolved in various ratios of LDAO and sodium cholate showed that the 873- to 780-nm transition in LDAO and cholate is also due to dissociation of the B873 into smaller units.

The bacteriochlorophyll-containing light-harvesting complexes of the chromatophore membrane of photosynthetic bacteria are responsible for the absorption and transfer of light energy to the photoreaction centers, which catalyze the primary process in energy transduction in photosynthesis [Clayton, 1978; see Cogdell and Thornber (1980)]. Many light-harvesting complexes from purple non-sulfur bacteria have now been isolated [Sauer & Austin, 1978; Cogdell et al., 1982; Picorel et al., 1983; Varga & Staehelin, 1985; see Zuber et al. (1985)]. They have been found to be of three principal types: LHC I, exhibiting an IR absorption maximum between 870 and 890 nm (designated B870/890);[1] LHC II, with ab-

[†] This work was supported by the Swiss National Science Foundation (Grant 3.313-0.82), the Hoffmann-La Roche Research Foundation, and an EMBO award (R.G.).
[‡] Dedicated to Prof. Dr. Hans Wanner on the occasion of his 70th birthday.
* Author to whom correspondence should be addressed.
[§] Institute for Plant Biology.
[∥] ETH-Zentrum.

[1] Throughout the text we refer to the B873 and B875 complex from *R. rubrum* G9+. These complexes are essentially identical: in some laboratories (including ours) the complex exhibits an absorption maximum at 873 nm, whereas in other laboratories an absorption maximum at 875 nm is apparently observed. It is generally believed that these small differences arise from a slight alteration of the parent genotype that has occurred in the years following its isolation and/or differences in the growth conditions used by various groups.

0006-2960/88/0427-1004$01.50/0

sorption at 800–850 nm (designated B800–850); and LHC III, with absorption at 800–820 nm (designated B800–820) [see Cogdell and Thornber (1980), Cogdell et al. (1984), Drews (1985), Zuber et al. (1985), and Bachofen and Wiemken (1986)]. *Rhodospirillum rubrum* S1 (wild-type) and its mutant strain G9+ (a carotenoid-less mutant) contain only the first type of antenna complex (designated B880 and B873, depending on the wavelength of the absorption maximum in *R. rubrum* S1 and G9+, respectively.[1] These complexes have been shown to contain two nonidentical polypeptides, α and β, two molecules of BChl,[2] and in addition in the wild-type strain one molecule of spirilloxanthin. After isolation, the complex contains 1–2 molecules of bound phospholipid (Picorel et al., 1983; Brunisholz et al., 1984a,b). The amino acid sequences have now been determined (Brunisholz et al., 1984a,b); however, the central question concerning the location of the bacteriochlorophyll binding site and the cause of the large red-shift of the absorption maximum from 770 nm for free BChl to about 870 nm as well as of the accompanying hyperchromicity is still not answered [see Scherz and Parson (1986)]. Furthermore, the minimal size of the functional unit of the light-harvesting complex is not known. In this study some of these questions are studied experimentally with the B873 complex from *R. rubrum* G9+. A preliminary report has been presented (Bachofen et al., 1987).

Materials and Methods

Lauryldimethylamine *N*-oxide (>90% pure) was obtained from Fluka, *N*-ethylmaleimide nitroxide was from Molecular Probes, and octyl β-D-glucoside (βOG) and octylpentakis(oxyethylene) (O-POE) were obtained from Bachem. All other reagents used were of analytical grade.

Isolation of the Light-Harvesting Complexes. Light-harvesting complexes (B873) were isolated from chromatophores of *R. rubrum* G9+ by the LDAO extraction method of Picorel et al. (1983) with the following modifications: for the final DEAE-cellulose chromatography step the extracted B873, dialyzed overnight against detergent-free buffer, was loaded onto a small column (1.5 cm × 6.0 cm) in 50 mM Tris-HCl, pH 8.0, and the column washed with 2 volumes of the same buffer containing 25 mM NaCl and 0.2% βOG. A first eluate was obtained with the same buffer containing 250 mM NaCl. B873 remaining bound to the column was eluted completely by buffer–NaCl (250 mM) containing 0.05% LDAO instead of 0.2% βOG. The eluates were dialyzed separately against 20 mM Tris-HCl, pH 8.0, for 2 days. All solutions were gassed with N_2 (>99% pure). All steps were performed in dim light. Protein determinations were performed by using the modified Lowry method of Peterson et al. (1977) to avoid interference by bacteriochlorophyll. The purity of the complexes was checked routinely by using SDS–PAGE with gels containing 12.5% and 18% acrylamide, respectively. The protein concentration of the dialyzed B873 was usually sufficient to perform most of the experiments described below. When necessary, however, the detergent-solubilized B873 was concentrated without extensive losses or changes in the absorption spectrum by using Centricon 10 concentrating tubes (Amicon). Detergent-free B873 was stored under nitrogen in the dark at 4 °C and was stable (as judged from the absorption spectrum and SDS gel profile) for several weeks in this form. Detergent solubilization of the dialyzed B873 was performed by the dropwise addition of the chosen detergent to a larger volume of sample. Detergent exchange was obtained by first dialyzing the initial detergent for 24 h as above followed by dialysis for a further 24 h against the detergent chosen using four changes of buffer. For the analytical ultracentrifugation experiments, detergent-free B873 (approximately 1 mg/mL protein) was dialyzed extensively against O-POE as described by Dorset et al. (1983) for the porin channel from *Escherichia coli* K12.

Absorption Spectroscopy. Absorption spectroscopy was performed with a Uvikon 810 spectrophotometer (Kontron Instruments) with the attachment for turbid samples. In no case did the contribution due to turbidity amount to more than about 2% of the total absorption at 600 nm. All spectra were taken with quartz 2-mm cuvettes (Hellma). For measurements performed over an extended period of time, the sample compartment was continually flushed with nitrogen. No photobleaching of the BChl was observed. Absorption spectra were digitized and then analyzed by fitting a sum of Gaussians to the chosen spectral region using an Apple II computer.

UV and Near-IR Circular Dichroism. UV CD measurements of detergent-free B873 and LDAO-solubilized B873 were performed by using a Jasco 500 spectrometer with temperature control for the sample holder. The cell compartment was flushed continually with N_2 during the measurement. All spectra are given as the average of two to three measurements after base-line subtraction. The UV CD data were fitted to their secondary structure components by using the reference data of Chen et al. (1974). CD measurements in the near-IR region were performed on a Jobin dichrograph or a Jasco 1000A, using a 5-mm path-length cell. The distance between the cell and the photomultiplier tube was varied as appropriate, and in some cases computer averaging was used to smooth the data.

Spin-Labeling of the Light-Harvesting Complexes. Detergent-free B873 was spin-labeled with *N*-ethylmaleimide *N*-oxide (NEM nitroxide) by the method of McConnell and Hamilton (1968). After extensive dialysis to remove the unbound spin-label, the samples were measured under conditions known to immobilize protein-bound spin-labels (see below). Such samples contained no measurable free label, nor did the sample buffer after the protein was removed by TCA precipitation. For some experiments bovine hemoglobin (a gift from Dr. E. Di Iorio, ETH-Zurich) was labeled under identical conditions and used as a standard for the calibration of rotational correlation time vs central line width.

Electron Spin Resonance (ESR) Measurements. ESR spectra were obtained with a Varian Century line 9-GHz spectrometer equipped with a Varian variable temperature accessory and a digital thermometer. For all measurements 100-kHz field modulation was used. The incident microwave power was 5 mW. The field sweep was 200 G and the modulation amplitude 1 G. In some cases for reasons of sensitivity a modulation amplitude of 5 G was used. Although this might be expected to produce some spectral distortion, under our conditions the distortion was minimal and did not affect the interpretation of the ESR data shown. Samples were filled into glass capillaries by use of a microsyringe and measured immediately. The capillary glass had a weak intrinsic ESR signal that produces the distorted base line observed. For some

[2] Abbreviations: LDAO, lauryldimethylamine *N*-oxide; SDS, sodium dodecyl sulfate; PAGE, polyacrylamide gel electrophoresis; O-POE, octylpentakis(oxyethylene); βOG, octyl β-D-glucoside; BChl, bacteriochlorophyll; BPh, bacteriopheophytin; Hb, hemoglobin; TID, 3-(trifluoromethyl)-3-(*m*-iodophenyl)diazirine; NEM, *N*-ethylmaleimide; Tris-HCl, tris(hydroxymethyl)aminomethane; DEAE, diethylaminoethyl; TCA, trichloroacetic acid. The designations B873/LDAO/cholate and B873/cholate/LDAO refer to a detergent-free B873 pigment–protein complex solubilized with the detergents given in the order of addition shown.

Scheme I: Detergent-Induced Transitions of the B873 Complex[a]

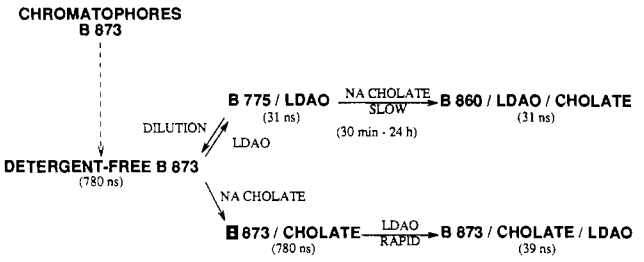

[a] Numbers shown in parentheses represent the apparent rotational correlation times calculated from the ESR data of spin-labeled complexes (see Figure 4).

cases base-line subtraction was performed to demonstrate that no nitroxide spin-label spin exchange mechanism was present. However, as a method to rapidly digitize spectra was not available and the slightly distorted base line has no significance for the measurements shown below, base-line subtraction was not done routinely.

Analytical Ultracentrifugation. Sedimentation studies were performed in a Beckman Model E analytical ultracentrifuge equipped with a photoelectric absorption scanning system. Absorption was recorded routinely at 280 or 360 nm, and a 12-mm double-sector cell (filled Epon) was used in all studies. No fluorocarbon oil was used because of the emulsifying effect of detergents. Sedimentation velocity experiments were performed by using an An-D rotor with protein solutions having an absorption of 0.1–0.5, at speeds of 26 000 rpm at 20 °C. Sedimentation equilibrium experiments were performed at similar protein concentrations at 20 °C by the meniscus depletion method (Yphantis, 1964). The base-line absorbance was determined by analysis of the data using a linear regression computer program (H. Berger, Biocenter, University of Basel, Switzerland) that adjusted the base line to obtain the best linear fit of ln A (absorbance) vs r^2 (radius). A partial specific volume ($\bar{v}$) of 0.73 cm^3/g was used for the protein in all calculations. The value used for $\bar{v}$ is typical for membrane proteins (Lustig and Rosenbusch, personal communication) and corresponds closely to that obtained from the amino acid composition for the α and β polypeptides, respectively.

Results

Purification of the Light-Harvesting Complexes. The LDAO extraction method developed for the light-harvesting complex of wild-type *R. rubrum* S1, according to Picorel et al. (1983), also worked out successfully for the carotenoid-less mutant *R. rubrum* G9+. It yielded a highly pure B873 containing only the two polypeptides α and β as observed by SDS–PAGE. The separation of the two polypeptides on SDS–gels is probably due to a conformational difference in the SDS micelles since their molecular weights are almost identical [6101 and 6079, respectively, as calculated from the amino acid sequences (Brunisholz et al., 1984a,b)]. When LDAO was used as the solubilizing agent, the absorption spectrum showed a minor absorption maximum at 775 nm that usually disappeared after dialysis against detergent-free buffer of low ionic strength. However, no BChl appeared in the dialysis buffer; thus, the change in the absorption spectrum seems to be due only to the absorption spectrum of the B873 (see below). This detergent-free B873 is relatively stable to high levels of illumination (not fluorescent lights) and to temperatures below 40 °C.

Detergent-Induced Spectral Changes of the Purified B873 Complex. Purified light-harvesting complexes show several unusual reversible changes in their absorption spectrum when

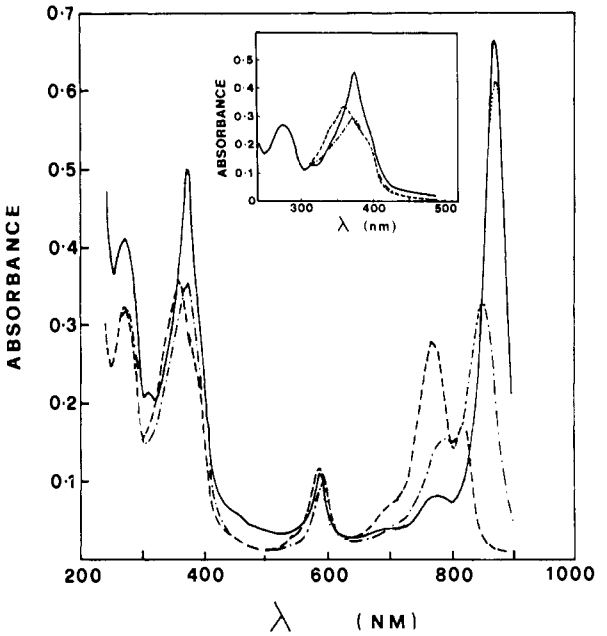

FIGURE 1: Absorption spectra of the detergent-free B873 before (—) and after (- - -) solubilization with 0.1% LDAO and following the further addition of 1% sodium cholate after 24 h (–·–). Also shown is a preparation of detergent-free B873 that had been made to 0.1% LDAO and then diluted immediately with buffer such that the final LDAO concentration was 0.001% (···). The initial absorption spectrum of the detergent-free sample can be restored completely (with the same BChl:protein ratio) by dialysis. Spectra were taken by using a 2-mm cuvette placed close to the photomultiplier and digitized (after correction for dilution) by using the software supplied with the instrument. The insert shows the Soret region after correction for residual light scattering (see Materials and Methods).

solubilized with either LDAO and/or sodium cholate (Scheme I, Figure 1).

Detergent-free B873 incubated with 0.1% LDAO rapidly lost the major absorption band at 873 nm, which was simultaneously replaced by a less intense band at 775 nm (Figure 1). This phenomenon is completely reversible: rapid dilution of LDAO-incubated B873, now absorbing at 775 nm and henceforth named B775, into detergent-free buffer (final LDAO concentration 0.007%) at room temperature restores the absorption peak at 873 nm almost instantaneously. Under the conditions given, 0.1% LDAO (corresponding to an LDAO/$\alpha\beta$ dimer molar ratio of approximately 300) was the lowest concentration sufficient to shift the 873-nm absorption to 775 nm. Addition of 0.5–1.0% sodium cholate to the LDAO-incubated complex (B775) caused a slow reversal of the LDAO-induced blue-shift, reaching an absorption peak at 860 nm only after several days. During the first 30 min when the largest changes of wavelength of the absorption maximum occur, no isosbestic point is observed. In contrast, in the initial reversal phase a number of *discrete transitory states* are observed, characteristically at 820–825 and 850 nm. Interestingly enough, reversal of the order of addition did NOT produce similar changes in the near-IR absorption spectrum. We believe that the reversibility of the dilution-induced 775- to 873-nm absorption transition is a good criterion of a *native* protein structure. Since this transition occurs only partially if at all when the solutions are aged, it was used routinely to determine the nativeness of the pigment–protein complexes. We emphasize that in all cases examined the dilution-induced absorption transition was paralleled by corresponding changes in the CD spectrum.

The reversibility of the spectral shift described allows the hyperchromic shift exhibited by the BChl chromophores of

Table I: Analysis of the Near-IR and Soret Spectral Region of the Light-Harvesting Complexes

	Soret region			near-IR region		
preparation	λ (nm)	σ^a (nm)	% total intensity	λ (nm)	σ^a (nm)	% total intensity
B873 (detergent-free)	376 (B_y)	18	76.3	873	17	74.9
	335 (B_x)	16	23.7	775	24	14.4
B775/LDAO	395 (B_y)	14	21.4	825	13	26.6
	260 (B_y')	18	55.2			
	320 (B_x)	16	23.4	775	20	73.4
B855/LDAO/cholate after 24 h	373 (B_y)	24	77.4	855	20	58.8
				820	14	10.5
	320 (B_x)	18	22.6	775	23	30.7

[a] σ is the half line width of a Gaussian line at wavelength λ.

the purified B873 to be quantified. Absorption spectra of the detergent-free B8738 B775/LDAO, and B855/LDAO/cholate and of B873, formed after dilution of B750/LDAO with buffer, preparations were analyzed by using a sum of Gaussians for wavelengths above 660 nm (corresponding to the Q_y transition). It was found that the absorption spectra of detergent-free B873 and B855/LDAO/cholate preparations could be fitted well by a sum of three Gaussian components, whereas those from preparations of B775/LDAO required only two components (Table I). In all cases a peak at 775 nm was observed in addition to a minor intermediate component between 815 and 834 nm. For the detergent-free B873 the minor component at 834 nm corresponded to less than 11% of the summed intensity of all three components. For the B775/LDAO and B855/LDAO/cholate forms the minor component corresponded to 26.6% and 10.5% of the total intensity, respectively. A large hypochromism was seen for the transition from 873 to 775 nm, the total intensity decreasing by two-thirds at 775 nm, while the hyperchromic increase in intensity observed for the LDAO/cholate complex (B855) was approximately 1.6.

Finally, it should be noted that the half line width (σ) for the 873 nm band is 15% narrower than that for the band at 775 nm. The changes in the Soret region do not show pronounced hyperchromic effects after correction for the effects of light scattering (Figure 1, insert), although such changes might not be observable since the oscillator strength of the Soret bands is at least 5 times greater than that of the Q_y band. Interestingly, however, the major spectral effect of LDAO in this region appears to cause a splitting of the B_y transition, which is reversed by the further addition of sodium cholate. This is the reverse of the changes observed in the near-IR region; there the three components of the Q_y transition are reduced to two by the addition of LDAO. Reappearance of a third component is induced by the further addition of sodium cholate.

Near-IR CD of the Isolated Light-Harvesting Complexes. Detergent-free B873 exhibited a near-IR-CD spectrum in the 500–1000-nm region with a positive peak at 863 nm, a crossover point at 870 nm, and a negative peak at 880 nm and is essentially identical with the B873 component in intact chromatophores (Figure 2b, insert). The small red-shift observed for the detergent-free B873 in comparison to the chromatophores is possibly due to the additional contribution from the reaction centers in the latter preparation. A further small trough was observed at 780 nm. For these measurements B873 was used directly from the final dialysis step of the preparation. These samples are probably finely dispersed particles and show very little scattering. For B873 preparations that are not homogeneously suspended, the low-wavelength trough at 880 nm is often no longer observable (Figure 2a). However, the CD spectra observed for both high- and low-scattering preparation after detergent solubilization were

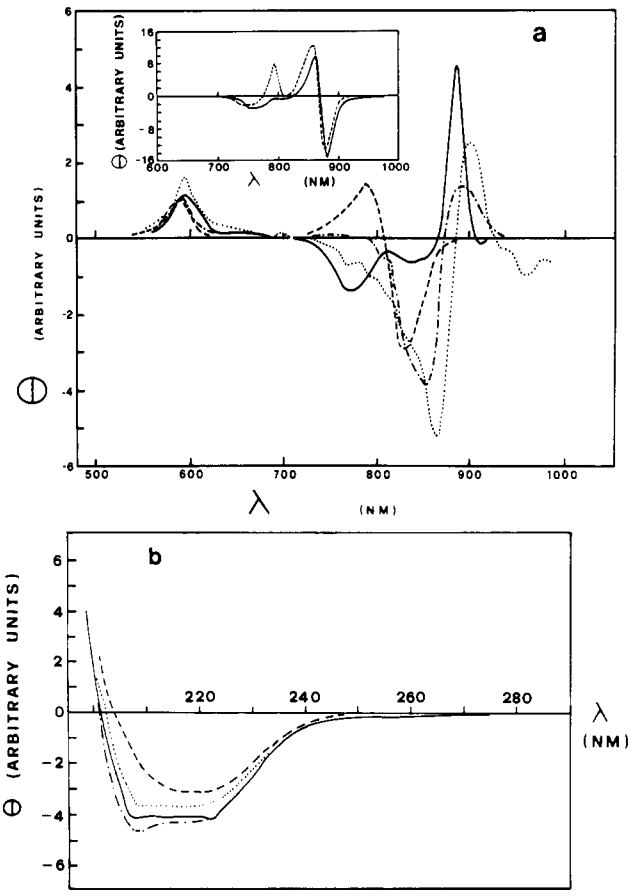

FIGURE 2: (a) Near-IR CD spectra of the detergent-free B873 (a) before (—) and (b) after (- - -) solubilization with 0.1% LDAO, (c) in 0.1% LDAO followed by 1% sodium cholate after 1 h (-·-), and (d) after 24 h (···). The spectrum of the detergent-free B873 solubilized initially with 1% sodium cholate followed by the addition of 0.1% LDAO was essentially identical with that of the B873 before detergent treatment. All spectra are shown after subtraction of the base line. The near-IR CD spectrum of the detergent-free B873 shown in the main figure was taken from a sample resuspended from a high-speed pellet. The loss of the trough at 860 nm (see insert) was due to scattering and could be reversed by sonication. The insert shows the near-IR CD spectrum of detergent-free B873 (—) taken directly from the last dialysis step, superimposed upon the near-IR CD spectrum of isolated chromatophores (- - -). For clarity the effects of the addition of LDAO and cholate are not shown but were identical with those shown in the main figure. (b) UV CD spectrum of the detergent-free B873 at 20, (—), 40, (···), and 80 °C (- - -). Also shown is the UV CD spectrum of the LDAO-solubilized B780 at 20 °C (-·-). Spectra were taken by using a 0.5-mm cell and with constant flushing of the cell compartment with N_2.

identical. Increasing the cell-to-photomultiplier distance from 2 mm to either 5 or 10 cm also absolished the peak at 870 nm, leaving the trough at 780 nm relatively unaffected. Incubation of detergent-free B873 with 0.1% LDAO led to a large increase of a peak at 780 nm with a subsequent loss of the signal at

Table II: Circular Dichroism of Light-Harvesting Complexes[a]

preparation	% α	% β	% R	SD
B873 (detergent-free)	42.6	16.4	41	0.318
B780/0.1% LDAO	43.1	18.5	38.5	0.28
B873 (40 °C)	47.6	28.6	23.8	0.228
B873 (60 °C)	50	27.3	22.7	0.237
B873 (80 °C)	62.5	36.8	0.7	0.36

[a] Analysis of the CD data shown in Figure 2 in terms of the components due to α-helix, β-sheet, and random coil (R) using the reference data of Chen et al. (1974). SD is the residual $\sigma(\text{exptl} - \text{calcd})/(N - 1)$ summed for all N.

860–880 nm. Further addition of sodium cholate to 1% led again to the appearance of an exciton band at 880 nm and a corresponding reduction of the intensity at 780 nm (Figure 2a). These changes appeared to vary linearly with the corresponding changes in absorption described above. Increasing the cell-to-photomultiplier distance from 2 mm to 5 or 10 cm had essentially no effect upon the near-IR CD spectra of the detergent-solubilized complexes. The spectrum of detergent-free B873 was unchanged when cholate was made to 1% or by the subsequent addition of LDAO (data not shown).

UV CD Spectra of Purified Light-Harvesting Complexes. It is possible to monitor detergent-induced changes of protein secondary structure by UV CD. Detergent-free B873 preparations are slightly turbid, necessitating the use of very thin cells (0.5 mm) to minimize the effect of light scattering. Subsequent sonication of the same sample had no observable effect upon the UV CD spectrum, which shows no spurious or anomalous bands usually attributed to the effects of light scattering (Mao & Wallace, 1984). Detergent-free B873 preparations at 20 °C exhibit a UV CD spectrum having double troughs of similar intensity at 222 and 208 nm (Figure 2b) and a peak at 190 nm (not shown). Analysis of the spectra using the reference data of Chen et al. (1974) yields values of 43%, 16.4%, and 41% for the α-helix, β-sheet, and random coil components, respectively (Table II). Solubilization of the detergent-free B873 with 0.1% LDAO led to only a very minor alteration of the CD spectrum, even below 200 nm. These small changes are probably accounted for by a reduction of the residual light scattering of the solution after solubilization.

The B873 secondary structure was observed to be extremely stable: up to 60 °C only small changes were detected, and only at 80 °C was a significant alteration observed. Interestingly, this did not correspond to an unfolding of the structure as is usually observed with water-soluble proteins; rather, the structure became more ordered with a 20% increase in α-helix and β-sheet components and an almost total disappearance of the random coil component compared to that observed at 20 °C.

Analytical Ultracentrifugation Measurements. Sedimentation velocity experiments of detergent-free B873 showed a predominance of large aggregates. Solubilization of the detergent-free B873 with 0.1% LDAO prior to centrifugation caused the protein to sediment as a single but broad peak with a sedimentation coefficient ($s_{20,w}$) of 4.1 S. The molecular weight of this complex is difficult to obtain by subsequent sedimentation equilibrium experiments since all components (solvent, protein, and protein–detergent micelles) of the buoyancy term $(1 - \Phi'\rho)$, where Φ' and ρ are the partial specific volume of the protein-detergent micelle and the density of the solvent, respectively, must be defined (Tanford et al., 1974). Rosenbusch and co-workers (Spiess et al., 1981) have recently introduced the nonionic detergent, octylpentakis(oxyethylene) (O-POE), that has a partial specific volume of $\bar{v}_d$ = 1.005 cm^3/g (i.e., $\bar{v}_d = 1/\rho$). Thus, sedimentation velocity experiments may be performed essentially as with water-soluble proteins, detergent binding affecting only the hydrodynamic radius of the protein. With this method it is not necessary to include the hydrodynamic radius explicitly. The molecular weights of the complexes solubilized with O-POE were obtained from a linear transformation of the sedimentation equilibrium data according to

$$M_r(1 - \bar{v}\rho) = (2RT/\omega^2)(\mathrm{d} \ln c/\mathrm{d}r^2) \qquad (1)$$

where M_r and $\bar{v}$ are the molecular weight and partial specific volume of the detergent-free protein, respectively, ω is the angular velocity (in radians per second), c is the concentration of the complex, and r is the distance from the rotor center [see also Ott et al. (1982)]. The molecular weight of the detergent–protein complex is given by (Spiess et al., 1981)

$$M_r^c(1 - \bar{v}_c\rho) = M_r[(1 - \bar{v}\rho) + \delta(1 - \bar{v}_d\rho)] \qquad (2)$$

where M_r^c and $\bar{v}_c$ are the molecular weight and partial specific volume of the protein–detergent complex (micelle) and δ is the weight of detergent bound per mole of protein. Because the detergent buoyancy term $\delta(1 - \bar{v}_d\rho)$ goes to zero, the molecular weight determined is identical with that of the detergent-free protein M_r.

Furthermore, O-POE is quite suitable for the solubilization of detergent-free B873: at 0.2% O-POE the near-IR absorption spectrum remains characteristic of "native" B873 (i.e, identical with that of detergent-free B873), whereas significant reversible losses of intensity at 873 nm were observed when the O-POE concentration is raised to 0.5%. Complete loss of the 873-nm peak was observed when the O-POE concentration was raised to 1.0%.

Sedimentation velocity experiments of B873 dissolved in 0.2% O-POE in 50 mM Tris-HCl, pH 8.0, revealed the presence of two distinct boundaries corresponding to aggregates of large molecular weight (>10^6) and a lower molecular weight component with a sedimentation coefficient of 1.56 S (Figure 3a). This distinctive pattern was observed for scanning wavelengths of either 280 (protein plus pigment) or 360 nm (pigment only). The aggregates contributed approximately 25% of the total intensity at 280 nm. When these data were combined with those obtained from sedimentation equilibrium experiments (Figure 3b), the 1.56-S fraction could be resolved into two low molecular weight species of approximately 37–40K and 24K, respectively. Species of very low molecular weight were not observed. When detergent-free B873 was dialyzed extensively against 1% O-POE, only protein species with molecular weights of 13K and 6K [probably corresponding to dimeric (α/β) and monomeric (α or β) states], respectively, were derived from the sedimentation equilibrium analysis (Table III). Since the sedimentation velocity experiment indicated the presence of two components, the nonlinear ln A vs r^2 plot could be fitted by two linear relations.

Table III: Ultracentrifugation Data of Light-Harvesting Complexes[a]

		species			
		mainly B873		B775	
0.2% O-POE	280	37.5–40K	17K		
	360	38K	24K		
1.0% O-POE	280			13.1K	5.7K
	360			9K	4.3K

[a] Detergent-free B873 were suspended in 50 mM Tris-HCl, pH 8.0, and then solubilized with O-POE as described and then used immediately. Sedimentation equilibrium runs were observed at 360 and 280 nm, characteristic of protein and bound chromophore, respectively. No unbound BChl could be detected in these experiments.

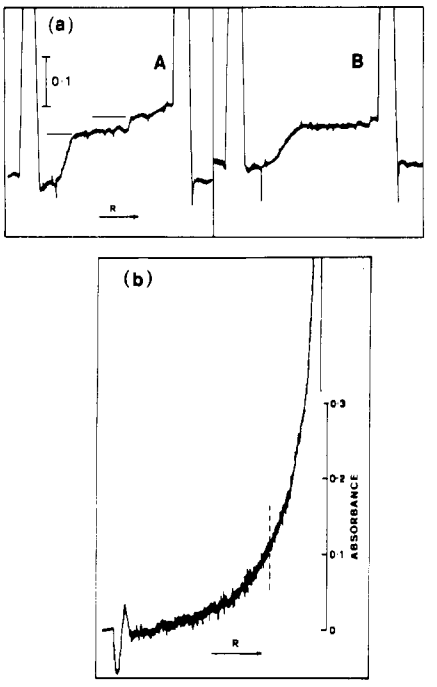

FIGURE 3: (a) Sedimentation velocity analysis of purified B873 solubilized in 50 mM Tris-HCl, pH 8.0, containing 0.2% O-POE. Sedimentation is from left to right, and the time points (A, 16 min; B, 64 min) are shown as representative. The rotor speed was 52000 rpm, and the running temperature was 22 °C. Absorbance was measured at 280 nm and is shown as a function of distance r (arbitrary units) from the rotor center. The heights of the two levels shown correspond to aggregates ($>10^6$) and low molecular weight species, respectively. They were used to calculate the relative weight ratios of the components. (b) Sedimentation equilibrium analysis of B873 dialyzed against the above buffer. Absorbance was monitored at 280 nm and is shown as a function of distance r. The rotor speed was 26000 rpm, and the running temperature was 20 °C. The insert shows the resolved ln A vs r^2 plots according to eq 1. Transformation of the raw data showed two distinct components, indicated by the dotted line, which could be resolved by an iterative regression procedure.

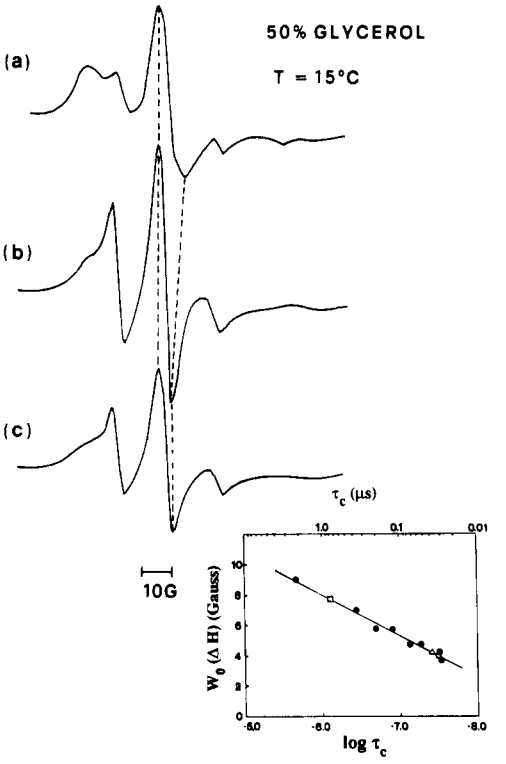

FIGURE 4: ESR first-derivative spectra of the NEM nitroxide labeled detergent-free B873 before (a) and after (b) solubilization with LDAO and sodium cholate/LDAO (c) at 15 °C in 50% glycerol. The arrows shown on the lowermost spectrum of the figure depict the central line width used for the calculation of the rotational correlation time. The insert shows the calibration curve of the apparent rotational correlation time of NEM nitroxide labeled Hb vs width of the central line (filled circles) determined by measuring the width between the central maximum and minimum of the first derivative spectrum. For the solid circles ESR spectra of NEM-labeled Hb were recorded in glycerol solutions and glycerol contents varying between 0 and 70%, and temperatures varied between +20 °C and −20 °C, respectively. The open circles represent data from spin-labeled B873 aggregates and B775/LDAO complexes, respectively, in 50% glycerol at 15 °C.

ESR Studies of Spin-Labeled Light-Harvesting Complexes. The effects of solubilization of nitroxide-labeled B873 complex with LDAO and sodium cholate were examined by electron spin resonance. The labeling procedure did not change the features of the optical absorption spectrum of the detergent-free B873 examined here.

ESR spectra of spin-labeled detergent-free B873 contained two distinct components characteristic of immobilized and freely rotating environments, respectively (Figure 4a). These effects paralleled those observed for the broad component (see below). The detergent conditions sufficient to produce changes in the ESR spectrum were similar to those that produced changes in the absorption spectra of the spin-labeled complexes (see Scheme I). Thus, the addition of 0.1% LDAO to detergent-free B873 induced extensive narrowing of both broad and narrow components (Figure 4b), which remained unchanged by 1% cholate. Addition of 1% cholate to detergent-free B873 had no effect, but the further addition of 0.1% LDAO under conditions where the absorption remained characteristic of detergent-free B873 rapidly induced an increased rate of averaging of the broad and narrow components (Figure 4c) similar to that observed when detergent-free B873 was solubilized with 0.1% LDAO.

Approximate correlation times of these complexes were deduced from a calibration curve obtained with spin-labeled hemoglobin (Hb) (see Appendix). If one assumes that the broad component observed for detergent-free B873 also corresponds to a tightly bound immobile spin-label, the effective correlation time for this complex was found to be 780 ns in 50% glycerol at 15 °C and decreased to 30–40 ns after solubilization with 0.1% LDAO. Within experimental error the effective correlation time for the B873/cholate/LDAO complex was in the same range as that of the B775/LDAO complex above. τ_c values of the detergent-solubilized LHC complexes remained proportional to viscosity for a single effective hydrodynamic radius (r) at all temperatures shown.

Discussion

The present study attempts to correlate detergent-induced changes of the near-IR absorption and the CD spectra of the isolated B873 complex from *R. rubrum* G9+ to molecular aggregation events of its component units.

Structural Elements Contributing to the Near-IR Absorption Spectrum. The B873 complex from *R. rubrum* G9+ has been shown to consist of two low molecular weight polypeptides (Cogdell et al., 1982; Picorel et al., 1983; Brunisholz et al., 1984a), both of which have been sequenced (Brunisholz et al., 1981, 1984a) and shown to possess a tripartite structure: a hydrophobic domain flanked by two hydrophilic domains (see Figure 5). Studies using limited proteolysis and chemical labeling have shown that both N-termini are accessible at the cytoplasmic face of the chromatophore membrane and that the polypeptides traverse the membranes only once (Wiemken et al., 1983; Brunisholz et al., 1984b, 1986). Recently, by use of the hydrophobic and nonspecific photolabel, TID, the hydrophobic domain indicated by the hydropathy plot has been

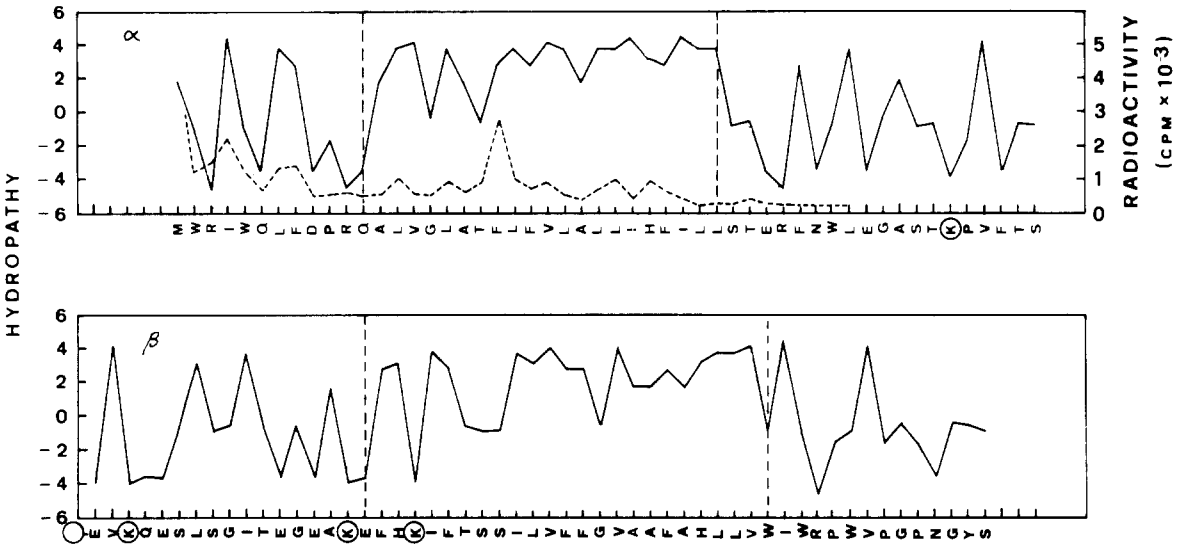

FIGURE 5: Hydropathy plot after Kyte and Doolittle (1982) of the α and β polypeptide sequences of the B873 complex. Possible labeling sites of the NEM nitroxide spin-label are ringed, and the dotted lines suggest the membrane-embedded domain. Also superimposed is the TID labeling pattern (also dashed) determined for the α polypeptide by Meister et al. (1985).

conformed experimentally (Meister et al., 1985; see Figure 5). In addition, the pattern of TID-labeled amino acids was found to be periodic, suggestive of a helical structure. Indeed, Theiler and Zuber (1984) have shown using ATR-IR spectroscopy that the B880 complex from *Rps. sphaeroides* contains significant α-helical secondary structure, and this assignment has been quantitated further in the present study for the carotenoid-less B873 complex. From the UV CD data it is calculated that the total complex contains 46% α-helix, essentially identical with data obtained by Breton and Nabedryk (1985) for the B875 and B800–850 complexes from *Rps. sphaeroides*. Assuming that approximately 50% of the α-polypeptide is present as α-helix (Meister et al., 1985), the percentage of α-helix observed for the intact B873 complex would be accounted for if the hydrophobic domain of the β-polypeptide were also present within the hydrocarbon layer as an α-helix, whereas the hydrophilic domains may possess no well-defined secondary structure. The domain assignment shown in Figure 5 places the conservative histidines, αHis-29 and βHis-37, at almost the same level in the bilayer closer to the periplasmic side, as has been suggested previously (Brunisholz et al., 1984a,b). These authors suggested that histidine residues form the fifth ligand for the magnesium atom of BChl. This suggestion is supported by proteolysis studies of the intact chromatophore membrane: even after extensive cleavage of the hydrophilic domains on the cytoplasmic side of the membranes, the local environment of the antennae BChl remains almost unaffected. In contrast with open sheet membranes of a mutant of *Rps. sphaeroides*, protease digestion resulted in rapid and extensive spectral changes (Wiemken & Bachofen, 1985).

The temperature dependence of the UV CD data (Table II) shows that the secondary structure of the isolated B873 complex is stable to 40–60 °C and is unaffected by solubilization with 0.1% LDAO. This suggests that the detergent-induced spectral changes reported here are not due to a general unfolding of the protein structure but are consistent with the dissociation of the oligomer as described below. However, small local changes of structure that are not observable by this technique may occur.

Of fundamental importance in describing the detergent-induced spectral changes is its correlation to the oligomeric state of the detergent-solubilized complexes. For the O-POE solubilized complexes, the analytical ultracentrifugation data show that dimeric ($\alpha\beta$) and monomeric (α or β) states are always associated with an absorption band at 775 nm. In contrast, the 873-nm absorption band is *always* observed with higher molecular weight oligomers (tetramers and hexamers, respectively) (Table III). Recently, Picorel et al. (1986) have examined the in situ structure of the B880 complex in a reaction-center-less mutant of *R. rubrum* using the radiation inactivation method. They concluded that both α and β bind BChl and that the $\alpha\beta$ dimer is reponsible for the absorption maximum at 880 nm. These results are not necessarily contradictory with our own. In our model, the building block of the minimal functional unit (λ_{max} = 873 nm) is the $\alpha\beta$-$BChl_2$ dimer, although the *isolated* species has an absorption maximum at 775 nm. Clearly, any disturbance of the basic $\alpha\beta$ exciton interaction will result in a perturbance of the multiple excitonic interactions necessary to generate the red-shift to 873 nm. Loach et al. (1985) have recently isolated an βOG-solubilized light-harvesting complex (λ_{max} = 820 nm) from the wild-type *R. rubrum* S1 that reversibly associates upon dilution to form a complex with an absorption maximum at 880 nm. The molecular weight of the complex was determined by means of gel exclusion chromatography in βOG to correspond to that of a tetramer (e.g., $\alpha_4\beta_4$). However, no corrections were made for the effect of detergent binding upon the hydrodynamic radius. We note that only 50 molecules of bound βOG per mole of $\alpha\beta$-dimer would be sufficient to generate a molecular weight of approximately 14.8K. In our studies using analytical ultracentrifugation we observe a small component at 820 nm when only monomers and dimers are present. We therefore prefer to leave the question of oligomeric structure of the B820/βOG form open until more detailed experiments can be performed.

For light-harvesting complexes solubilized with LDAO and sodium cholate, the situation is more complex. The ESR data show that addition of 0.1% LDAO (with concomitant appearance of the 775-nm absorption) leads to a dramatic increase in the signal intensity from a rapidly rotating component, although at least 20–30% of the total intensity is contributed by an immobilized component as judged by an appropriate integration of the two components. The broadening of the signal observed for the immobilized component is determined by the overall tumbling of the protein–detergent

micelle, and the apparent correlation time (τ_c) of the B775/LDAO complex is approximately 35 ns in 50% glycerol at 15 °C. Substitution of this value into eq 4 yields a hydrodynamic radius of 17 Å, which is similar to the value of 21 Å determined by Scherz and Parson (1984a) for small LDAO micelles in the presence of BPh and 20% acetic acid. This corresponds to approximately 50–70 LDAO monomers/micelle. From the calculated correlation times it appears that the B775/LDAO and B873/cholate/LDAO are approximately identical in size. By inference with the above studies with O-POE and the near-IR CD data, we suggest that LDAO dissociates the B873 into monomers (α-BChl and β-BChl) and dimers [$\alpha\beta$(BChl)$_2$] (see below). The ESR data show clearly that sodium cholate alone does not dissociate the B873 aggregate, whereas upon further addition of LDAO there is an immediate dissociation of the aggregate (as judged from the ESR spectra) to form small complexes of *approximately* similar size to those of B775/LDAO.[3] The near-IR absorption spectra remain unaffected after this dissociation step (see Scheme I). However, with the methods used it is not possible to distinguish between tetramers and dimers, and we suggest that the B873/cholate/LDAO complexes are probably tetramers/hexamers, stabilized by sodium cholate. Similarly, the addition of sodium cholate to B775/LDAO would cause LDAO-solubilized dimers to reassociate at a rate limited by the exchange processes between mixed micelles.

Any explanation of these effects must take into account the following three observations: (a) Formation of the B873 spectral form from dissociated α or β monomers containing bound pigment always leads to a hyperchromic absorption of the BChl. (b) The 873-nm band is red-shifted relative to that of free BChl. (c) The LDAO-solubilized complex (B775) exhibits a nonconservative exciton near-IR CD spectrum that becomes hyperchromic and red-shifted upon transformation of the B860–B870 complex by the addition of sodium cholate. Although the formation of an exciton dimer between pairs of BChl molecules is generally accepted [see Norris and Katz (1978)], it is well-known [see Cantor and Schimmel (1980)] that excitonic interaction formation does not lead to hyperchromicity. A further suggestion that the proximity of a charged group to the BChl moiety could lead to the 100-nm red-shift observed (Eccles & Honig, 1983; Brunisholz et al., 1984a) has been considered to be unlikely in a recent discussion by Scherz and Parson (1984a,b). Instead, on the basis of results obtained with BChl and BPh oligomers formed with micelles of LDAO, Scherz and Parson (1984a,b) have proposed a theory of "intensity borrowing" to explain the hyperchromicity and red-shift. In this theory the close proximity and geometry of chromophores allows a mixing of wave functions corresponding to the Q_x and Q_y transition dipoles of the near-IR region and the B_x and B_y transition dipoles of the Soret region, such that intensity from the latter can be "borrowed" to enhance the Q_x and Q_y transitions. In general our data are in agreement with the intensity borrowing theory of Scherz and Parson (1984b), although the detailed changes in the near-IR and Soret regions observed and calculated by the latter authors for their model system are somewhat different from those obtained here. In particular, although the hypochromism observed for the 873- to 775-nm transition is rather large, we observe almost no corresponding hyperchromism in the Soret region. This may be due to a combination of two reasons: (a) oscillator strengths of the B_x and B_y dipole moments of approximately 5-fold less than those for the Q_x and Q_y; (b) uncertainties in the correction for light scattering. Thus, for a decrease in intensity of two-thirds for the 873- to 775-nm transition only a 40% increase in intensity of the Soret region might be expected. This difference is not clearly observable in our data (Figure 1), which may arise from the uncertainties in our empirical correction for light scattering in this region. For the 775- to 855-nm transition, where the differences in light scattering are almost negligible, a 10% decrease in intensity in the Soret region is indeed observed, which compares well with the expected value of 12%.

It should be noted, however, that the Tinoco–Scherz and Parson treatment is based on a point–dipole approximation of the exciton interaction matrix elements and neglects charge-transfer transitions. These become serious approximations when the interacting molecules are close together. A rationalization of our data with the theory of Scherz and Parson (1984b) must await further detailed model calculations.

The reversal of the LDAO-induced 873- to 780-nm transition by cholate shows several interesting features. First, the spectral transition is slow (minutes to hours), and several distinct *intermediate states* are observed. This is consistent with the suggestion that the red-shift and hyperchromicity of the absorption spectrum of the native complex are due to oligomer/aggregate formation, oligomers of intermediate size ($37K > n > 13K$) thus showing characteristic spectral properties. Second, at the end point (i.e., after 24 h at 4 °C) the near-IR absorption spectrum can be resolved into three principal components, although those above 780 nm are shifted approximately 20 nm to the blue with respect to those in the original detergent-free B873 preparation. The hyperchromicity of the 855-nm band is only half that of the 873-nm band of the native complex. Although this suggests that the size of the oligomer may be smaller than the original functional unit which forms the B873 species, it seems likely that an alteration of the final geometry may also be involved.

The structural interpretation of these data is clarified by the near-IR CD data. An important observation is that the LDAO-solubilized B775 complex exhibits a nonconservative IR CD spectrum with a trough at the peak of the absorption spectrum. Since the ultracentrifuge data show that the appearance of a 780-nm form is always correlated with the presence of dimers and monomers in O-POE, the simplest interpretation of the near-IR CD data is that it corresponds to an $\alpha\beta$ dimer solubilized in LDAO micelles with the Q_y transition dipole moments aligned antiparallel to each other. The ultracentrifuge data (Table III) clearly show that the complex absorbing at longer wavelengths always corresponds to oligomers (tetramers and possibly hexamers), so it seems reasonable to suggest that the effect of cholate addition to the LDAO-solubilized B775 dimer is to cause the association of dimers, possibly through a specific charge interaction. It may be recalled that the composition of the chromatophore membranes consists of at least 20% charged lipids, PG, and cardiolipin (DaPra et al., 1982). Two to three dimers may form an oligomer with the Q_y transition dipole moments at each "side" of the elementary dimer structural unit aligned, leading to a red-shift and hyperchromic absorption according to the intensity borrowing theory described by Scherz and Parson (1984a,b). In this arrangement the Q_x transition dipole moments would not show a red-shift or hyperchromicity upon oligomerization, as is observed.

[3] In the analysis of the ESR data we equate an increase in the rotational diffusion with a dissociation of the complex. This interpretation is supported both by the location of the reactive amino groups and by analogy to the ultracentrifugation data obtained for O-POE complexes. Strictly speaking, however, an increase in the hydrophilic tail motion without complex dissociation remains a possibility.

The near-IR CD spectra of the detergent-free B873 or B873/LDAO/cholate complex may be explained largely by excitonic interactions between two or three [$\alpha\beta$(BChl)$_2$] dimers. (We choose to call this a *double-exciton* interaction since the BChl molecules within the dimer themselves participate in an intradimeric interaction.) This would be consistent with the cholate-induced red-shift of the 780-nm exciton, and the signal centering at 873 nm would correspond to that observed for intact chromaphores. The physical interpretation of the double-exciton model proposed here would be as follows. The presence of sodium cholate stabilizes the B873 functional unit solubilized with 0.1% LDAO, preventing its further dissociation into component subunits. Association of these units to form an array, such as in the detergent-free B873 complex, possibly induces a conformational change that reduces the CD band at 870 nm. We are presently investigating these ideas with isolated oligomers of defined size. However, the size of the "functional unit" observed in different detergents may not necessarily be uniform. Finally, it should be noted that we have not explicitly considered a charge-induced red-shift as causing the 780- to 873-nm transition. While this may also contribute to the red-shift, we believe that the present data point to the formation of multiple excitonic interactions as described by Scherz and Parson (1984b) as the principal causal event. In addition, a charge-induced red-shift cannot lead to hyperchromicity.

Detailed Structural Changes of the B873 Complex during Solubilization. The ESR data not only show that the solubilizing effect of LDAO and sodium cholate upon the B873 complex are in good agreement with the ultracentrifuge data performed in O-POE but also give insight into the detailed structural events occurring. The ESR spectra obtained for the NEM nitroxide labeled, detergent-free B873 were characteristic of two motional environments, corresponding to immobilized and freely rotating spin-labels, respectively. These terms should be considered with caution since detailed interpretation of the motion would require spectral simulation. The spectra presented resemble published spectra of spin-labeled hemoglobin (McConnell & Hamilton, 1968) under conditions where the apparent rotational correlation times of the two systems were comparable. For hemoglobin it has been shown that the NEM label binds to two cysteine sulfhydryl groups (McConnell & Hamilton, 1968), one of which is immobilized in a hydrophobic cleft and the other freely rotating at the protein surface (Moffat, 1971). Examination of the amino acid sequences of the α and β polypeptides of the light-harvesting complex (Figure 5) shows that although no cysteine is present, there are four lysine residues and a single N-terminal amino group that are possible candidates for covalent modification. The assignment of the membrane-bound domains suggests that the lysine residues may be partitioned in both hydrophilic and hydrophobic environments, the latter located within the membrane hydrocarbon layer and possibly packed between the α-helical segments of the $\alpha\beta$ dimer (βLys-16 and βLys-20) and the former present at the polar interface. Indeed, ^{19}F NMR (Ghosh et al., 1984) and ^{2}H NMR (unpublished data) of whole chromatophores suggest that the phenylalanine residues, which are present almost exclusively within the hydrocarbon region, are immobilized on the microsecond time scale. It seems likely that the lysines in this region might be subject to the same motional restrictions. These conclusions appear to be true also for the aggregate formed for the detergent-free B873 complex. It should be noted in this context that aggregate formation is *ordered* since it leads to a reconstitution of the native absorption spectrum and the suspensions are only very slightly turbid. It is clear that only a small fraction of rapidly averaging label is observed for the detergent-free B873 complex but that a similar fraction of mobile components is produced during formation of the B775/LDAO and B873/cholate/LDAO complexes. Examination of the sequences of α and β (Figure 5) shows that the β-N-terminus and lysines α47 and β3 are present at the free ends of the sequences. It is tempting, therefore, to suggest that at least part of these domains are not involved in dimer/tetramer/hexamer formation but only in long-range interactions with neighboring functional units.

Summary and Possible Physiological Significance. For the B873 complex the following conclusions hold: (a) The 873- to 775-nm transition is accompanied by a dissociation of the functional unit size (24–37K) and for complexes retaining their native structure this process is reversible. (b) Treatments that do not affect the main absorption band at 873 nm may nevertheless cause a dissociation of the isolated complex into its functional units. (c) The near-IR CD spectra are only indicative of the local environment of the BChl molecules and are weakly dependent upon the oligomeric structure of the complex. (d) Reversible dissociation of the isolated complex is accompanied by an increase in the local freedom of some domains, probably the hydrophilic regions.

One of the puzzling features of the light-harvesting complexes isolated so far from purple non-sulfur bacteria is that despite their similar structure and high homology a range of near-IR absorption peaks between 850 and 910 nm are observed. We exclude here the additional absorption maximum at 800 nm that corresponds to an additional BChl molecule at a nonhomologous site found in B875 and B850 (Clayton & Clayton, 1981; Kramer et al., 1984a,b). Even for a single type of light-harvesting complex (e.g., B873) an appropriate choice of detergent conditions (see Figure 1) can induce a distribution of absorption maxima that correspond to different oligomeric states and probably different relative geometries of the BChl molecules. We suggest that the different absorption maxima observed for various light-harvesting complexes may be rationalized by postulating that for a common functional unit only small changes in geometry of the functional unit of the $\alpha\beta$ dimer are necessary to induce the range of absorption maxima that are required for in vivo function in various organisms.

A Note on Nomenclature. Recently, Cogdell et al. (1985) have suggested that the term B875 complex should be used to denote light-harvesting complexes with an absorption maximum at 875 nm. From the foregoing experiments it is clear that this nomenclature can only be used for complexes in vivo since both detergent-free B875 and B875/cholate/LDAO forms correspond to the B875 complex, although they represent different molecular forms. We therefore suggest that the aggregation state should be added. The resolved functional unit with an absorption maximum at 875 nm would then be called the B875 oligomer and arrays formed from several functional units the B875 complex.

Acknowledgments

We thank Profs. J. Breton and J. Rosenbusch for stimulating discussions and A. Lustig for expert technical assistance with the ultracentrifugation measurements. We further thank Prof. J. Breton for the use of the CD spectrometer.

Appendix

For single-component ESR spectra, the rotational correlation time (τ_c) in the fast tumbling regime (10^{-11}–10^{-9} s) may be determined by the equation

$$\tau_c = (6.5 \times 10^{-10})\Delta H[(H_0/H_{-1})^{1/2} - 1] \quad \text{(s)} \qquad (3)$$

where ΔH is the peak-to-peak width of the central-field line in gauss and H_0 and H_{-1} are the peak-to-peak heights of the central-field and high-field lines, respectively (Stone et al., 1965). Unfortunately, the above equation cannot be used to derive correlation times τ_c for the immobilized component present in the spectra shown in Figure 4a. We have therefore developed a simpler and empirical analysis of the spectra to estimate the effective correlation times of the detergent-solubilized complexes.

Hemoglobin (Hb) labeled under conditions identical with those for B873 also exhibits two-component ESR spectra, which for appropriate solvent viscosities yield ESR spectra comparable to those shown in Figure 4 (data not shown). It has been established (McConnell & Hamilton, 1968) that Hb binds 2 mol of NEM spin-label/mol of protein, and X-ray crystallography studies have shown that one of these spin-labels is firmly bound to a protein crevice, whereas the other is freely rotating (Moffat, 1971). As the maximum width of the central-field line (ΔH) is always clearly observable and must be dependent upon the slowest τ_c (due to incomplete averaging of the tightly bound label by overall tumbling of the molecule at low solvent viscosities), it was possible to construct a calibration curve of ΔH vs τ_c for spin-labeled Hb (Figure 4, insert). Effective correlation times were obtained from the solvent viscosity by substituting the known hydrodynamic radius (29 Å) of Hb into the diffusion equation for a spherical molecule tumbling isotropically

$$\tau_c = (4/3)\pi r^3 \eta / 3kT \qquad (4)$$

where η is the viscosity in poise and r is the hydrodynamic radius in angstroms. Over the range of viscosities examined, ΔH vs log τ_c was found to be approximately linear. A possible difficulty with this approach would arise if the g anisotropy tensor (which determines the magnitude of ΔH) were strongly temperature dependent. In practice this appears not to be the case and was subsequently ignored for the calculation of τ_c.

REFERENCES

Bachofen, R., & Wiemken, V. (1986) *Encycl. Plant Physiol., New Ser. 19*, 620–631.

Bachofen, R., Ghosh, R., & Schwerzmann, R. (1987) *Prog. Photosynth. Res., Proc. Int. Congr. Photosynth., 7th, 1986 2*, II.1.21–24.

Breton, J., & Nabedryk, E. (1984) *FEBS Lett. 176*, 355–359.

Brunisholz, R. A., Cuendet, P. A., Theiler, R., & Zuber, H. (1981) *FEBS Lett. 129*, 150–153.

Brunisholz, R. A., Suter, F., & Zuber, H. (1984a) *Hoppe-Seyler's Z. Physiol. Chem. 365*, 675–688.

Brunisholz, R. A., Wiemken, V., Suter, F., Bachofen, R., & Zuber, H. (1984b) *Hoppe-Seyler's Z. Physiol. Chem. 365*, 689–701.

Brunisholz, R. A., Zuber, H., Valentine, J. G., Woolley, K. J., & Cogdell, R. J. (1986) *Biochim. Biophys. Acta 849*, 295–303.

Canaani, O. D., & Sauer, K. (1978) *Biochim. Biophys. Acta 501*, 545–553.

Cantor, C. R., & Schimmel, P. R. (1980) *Biophysical Chemistry*, p 395, W. H. Freeman, San Francisco.

Chen, Y. H., Yang, J. J., & Martinez, H. M. (1974) *Biochemistry 13*, 3350–3359.

Clayton, R. K. (1978) in *The Photosynthetic Bacteria* (Clayton, R. K., & Sistrom, W. R., Eds.) pp 387–396, Plenum, New York.

Clayton, R. K., & Clayton, B. J. (1981) *Proc. Natl. Acad. Sci. U.S.A. 78*, 5583–5587.

Cogdell, R. J., & Thornber, J. P. (1980) *FEBS Lett. 122*, 1–8.

Cogdell, R. J., & Scheer, H. (1985) *Photochem. Photobiol. 42*, 669–678.

Cogdell, R. J., Lindsay, J. G., Valentine, J., & Durant, I. (1982) *FEBS Lett. 150*, 151–154.

Cogdell, R. J., Zuber, H., Thornber, J. P., Drews, G., Gingras, G., Niederman, R. A., Parson, W. W., & Feher, G. (1985) *Biochim. Biophys. Acta 806*, 185–186.

DaPra, E., Snozzi, M., & Bachofen, R. (1982) *Arch. Microbiol. 133*, 23–27.

Dorset, D. L., Engel, E., Haener, M., Masalski, A., & Rosenbusch, J. P. (1983) *J. Mol. Biol. 165*, 701–710.

Drews, G. (1985) *Microbiol. Rev. 49*, 59–70.

Drews, G., Kaufmann, N., & Klug, G. (1985) in *Molecular Biology of the Photosynthetic Apparatus* (Steinback, K., et al., Eds.) pp 211–222, Cold Spring Harbor Laboratory, Cold Spring Harbor, NY.

Eccles, J., & Honig, B. (1983) *Proc. Natl. Acad. Sci. U.S.A. 80*, 4959–4962.

Ghosh, R., Bachofen, R., & Hauser, H. (1984) *FEBS Lett. 188*, 107–111.

Kramer, H. J. M., Van Grondelle, R., Hunter, C. N., Westerhuis, W. H. J., & Amesz, J. (1984a) *Biochim. Biophys. Acta 765*, 156–165.

Kramer, H. J. M., Pennoyer, J. D., Van Grondelle, R., Westerhuis, W. H. J., Niederman, R. A., & Amesz, J. (1984b) *Biochim. Biophys. Acta 767*, 335–344.

Kyte, J., & Doolittle, R. F. (1982) *J. Mol. Biol. 157*, 105–132.

Loach, P. A., Parkes, P. S., Miller, J. F., Hinchigen, S., & Callahan, P. M. (1985) in *Molecular Biology of the Photosynthetic Apparatus* (Steinback, K. E., et al., Eds.) pp 197–209, Cold Spring Harbor Laboratory, Cold Spring Harbor, NY.

Mao, D., & Wallace, B. A. (1984) *Biochemistry 23*, 2667–2673.

McConnell, H. M., & Hamilton, C. L. (1968) *Proc. Natl. Acad. Sci. U.S.A. 60*, 776–781.

Meister, H. P., Bachofen, R., Semenza, G., & Brunner, J. (1985) *J. Biol. Chem. 260*, 16326–16331.

Moffat, J. K. (1971) *J. Mol. Biol. 55*, 135–146.

Norris, J. R., & Katz, J. J. (1978) in *The Photosynthetic Bacteria* (Clayton, R. K., & Sistrom, W. R., Eds.), pp 397–418, Plenum, New York.

Ott, P., Lustig, A., Brodbeck, U., & Rosenbusch, J. P. (1982) *FEBS Lett. 138*, 187–189.

Peterson, G. L. (1977) *Anal. Biochem. 83*, 346–356.

Picorel, R., Bélanger, G., & Gingras, G. (1983) *Biochemistry 22*, 2491–2497.

Picorel, R., L'Ecuyer, A., Potier, M., & Gingras, G. (1986) *J. Biol. Chem. 261*, 3020–3024.

Riggs, A. (1961) *J. Biol. Chem. 236*, 1948–1954.

Sauer, K., & Austin, L. A. (1978) *Biochemistry 17*, 2011–2019.

Scherz, A., & Parson, W. W. (1984a) *Biochim. Biophys. Acta 776*, 653–665.

Scherz, A., & Parson, W. W. (1984b) *Biochim. Biophys. Acta 766*, 666–678.

Scherz, A., & Parson, W. W. (1986) *Photosynth. Res. 9*, 21–32.

Spiess, M., Hauser, H., Rosenbusch, J. P., & Semenza, G. (1981) *J. Biol. Chem. 256*, 8977–8982.

Stone, T. J., Buckman, T., Nordio, P. L., & McConnell, H. M. (1965) *Proc. Natl. Acad. Sci. U.S.A. 54*, 1011–1017.

Tanford, C., Nozaki, Y., Reynolds, J. A., & Makino, S. (1974) *Biochemistry 13*, 2369–2376.

Theiler, R., & Zuber, H. (1984) *Hoppe-Seyler's Z. Physiol. Chem. 365*, 721-729.
Tinoco, I., Jr. (1962) *Adv. Chem. Phys. 4*, 113-157.
Varga, A. R., & Staehlin, L. A. (1985) *J. Bacteriol. 161*, 921-927.
Wiemken, V., & Bachofen, R. (1982) *Biochim. Biophys. Acta 681*, 72-76.
Wiemken, V., & Bachofen, R. (1985) *Physiol. Veg. 23*, 789-800.
Wiemken, V., Brunisholz, R., Zuber, H., & Bachofen, R. (1983) *FEMS Lett. 16*, 297-301.
Yphantis, D. A. (1964) *Biochemistry 3*, 297-317.
Zuber, H. (1986) *Encycl. Plant Physiol., New Ser. 19*, 238-251.
Zuber, H., Sidler, W., Füglistaller, P., Brunisholz, R., & Theiler, R. (1985) in *Molecular Biology of the Photosynthetic Apparatus* (Steinback, K. E., et al., Eds.) pp 183-196, Cold Spring Harbor Laboratory, Cold Spring Harbor, NY.

Nitric Oxide Adducts of the Binuclear Iron Site of Hemerythrin: Spectroscopy and Reactivity†

Judith M. Nocek and Donald M. Kurtz, Jr.*
Department of Chemistry, Iowa State University, Ames, Iowa 50011
J. Timothy Sage, Yao-Min Xia, and Peter Debrunner
Department of Physics, University of Illinois, Urbana, Illinois 61801
Andrew K. Shiemke, Joann Sanders-Loehr, and Thomas M. Loehr
Department of Chemical and Biological Sciences, Oregon Graduate Center, Beaverton, Oregon 97006
Received June 16, 1987; Revised Manuscript Received October 2, 1987

ABSTRACT: Nitric oxide forms adducts with the binuclear iron site of hemerythrin (Hr) at [Fe(II),Fe(II)]deoxy and [Fe(II),Fe(III)]semimet oxidation levels. With deoxyHr our results establish that (i) NO binds reversibly, forming a complex which we label deoxyHrNO, (ii) NO forms a similar but distinct complex in the presence of fluoride, which we label deoxyHrFNO, (iii) NO is directly coordinated to one iron atom of the binuclear pair in these adducts, most likely in a bent end-on fashion, and (iv) the iron atoms in the binuclear sites of both deoxyHrNO and deoxyHrFNO are antiferromagnetically coupled, thereby generating unique electron paramagnetic resonance (EPR) detectable species. The novel EPR signal of deoxyHrNO (deoxyHrFNO) with $g_{\|} = 2.77$ (2.58) and $g_{\perp} = 1.84$ (1.80) is explained by the magnetic interaction of the Fe(II) ($S' = 2$) and $\{FeNO\}^7$ ($S = {}^3/_2$) centers observed by Mössbauer spectroscopy. Antiferromagnetic coupling leads to a ground state of $S^{eff} = {}^1/_2$. Analysis of the EPR parameters using the isotropic spin-exchange Hamiltonian, $\hat{H}_{ex} = 2J\hat{S}_{3/2'}\hat{S}_2$, and including zero-field splitting leads to a coupling constant, $-J \sim 23$ cm^{-1}, for deoxyHrNO. The resonance Raman spectrum of deoxyHrNO shows features at 433 and 421 cm^{-1} that shift downward with $^{15}N^{16}O$ and that are assigned to stretching and bending modes, respectively, of the $\{FeNO\}^7$ unit. Sensitivity of the bending mode to D_2O suggests that bound NO participates in hydrogen bonding. We propose that the terminal oxygen atom of NO is hydrogen bonded to the proton of the μ-hydroxo bridge in the Fe-(OH)-Fe unit. A bent Fe-N-O geometry is supported by spectroscopic and structural comparisons to synthetic complexes and is consistent with a limiting [Fe^{II},$Fe^{III}NO^-$] formulation for deoxyHrNO. Reversibility of NO binding to deoxyHr is demonstrated by bleaching of the optical and EPR spectra of deoxyHrNO upon additions of excess N_3^- or CNO^-. DeoxyHrNO undergoes autoxidation under anaerobic conditions over the course of several hours. The product of this autoxidation appears to be an EPR-silent NO adduct of semimetHr. The formal one-electron oxidations of the binuclear iron site of deoxyHr by NO and by HNO_2 can conceivably occur with no net change in charge on the iron site. In contrast, autoxidation of oxy- to metHr requires a change in net charge on the iron site, which may provide a kinetic barrier.

The non-heme iron oxygen-carrying protein hemerythrin (Hr),[1] which is found in several phyla of marine invertebrates, poses evolutionary, physiological, and biochemical contrasts to the more widespread heme oxygen carriers (Wilkins & Harrington, 1983; Klotz & Kurtz, 1984; Kurtz, 1986). Hemerythrins from erythrocytes of sipunculan worms usually consist of octamers ($M_r \sim 108\,000$) of essentially identical subunits. Each subunit contains a binuclear iron site that reversibly binds one molecule of O_2. The structure of this site in the azide adduct of [Fe^{III},Fe^{III}]metHr (metHrN_3) was determined by X-ray crystallography (Stenkamp et al., 1984; Sieker et al., 1982):

† This research was supported by grants from the National Institutes of Health (D.M.K., GM 37851; P.D., GM 16406; T.M.L. and J.S.-L., GM 18865).
* Address correspondence to this author at the Department of Chemistry, University of Georgia, Athens, GA 30602.

[1] Abbreviations: Hr, hemerythrin; deoxyHr, deoxyhemerythrin; metHr, methemerythrin; deoxyHrNO, NO adduct of deoxyHr; deoxyHrFNO, NO adduct of deoxyHr in the presence of excess fluoride; Tris, tris(hydroxymethyl)aminomethane; EDTA, ethylenediaminetetraacetate; OAc, acetate; $HBpz_3$, tri-1-pyrazolylborate; EPR, electron paramagnetic resonance.

0006-2960/88/0427-1014$01.50/0